Incommensurate magnetism in cuprate materials

F. Mancini* and D. Villani
Dipartimento di Scienze Fisiche ''E.R. Caianiello'' e Unità INFM di Salerno, Università di Salerno, 84081 Baronissi, Salerno, Italy

H. Matsumoto
Department of Applied Physics, Seikei University, Tokyo 180, Japan
(Received 25 June 1997)

In the low-doping region, an incommensurate magnetic phase is observed in $La_{2-x}Sr_xCuO_4$. By means of the composite-operator method we show that the single-band two-dimensional Hubbard model reproduces with good accuracy the experimental situation. In the higher-doping region, where experiments are not available, the incommensurability is depressed owing to the van Hove singularity near the Fermi level. By changing doping, the calculated incommensurability amplitude and the experimental critical temperature evolve in a similar way, suggesting a close relation between superconductivity and incommensurate magnetism. [S0163-1829(98)07109-4]

I. INTRODUCTION

The dynamical spin susceptibility for cuprate materials has been investigated by inelastic neutron scattering and NMR techniques. Neutron-scattering data on $La_{2-x}(Ba,Sr)_xCuO_4$ have shown[1–8] that away from half filling the commensurate antiferromagnetic phase is suppressed and short-range incommensurate antiferromagnetism develops. The magnetic Bragg peak in the dynamical structure factor $S(\mathbf{k},\omega)$ broadens and develops a structure with four peaks located at $[(1\pm\delta)\pi,\pi]$ and $[\pi,(1\pm\delta)\pi]$. The incommensurability amplitude $\delta(x)$ does not depend on the frequency and temperature; it is zero up to the doping $x\approx 0.05$ where a commensurate-incommensurate transition is observed; then, it increases with the hole concentration x, following the linear law $\delta(x)\approx 2x$ up to $x\approx 0.12$; beyond this point there is a deviation downward.[7,8] Unfortunately, experimental data above $x=0.20$ are not available due to the difficulty in preparing single crystals. It is important to stress[5] that the value of doping $x=0.05$, where the transition is observed, corresponds to the value of doping where the material becomes superconducting. These incommensurate spin fluctuations with a very large energy scale are not observed in other cuprate materials; a flat-topped magnetic peak has been observed[9] in $YBa_2Cu_3O_{6+y}$ with $y\approx 0.6$, while for the case of the electron-doped $Nd_{2-x}Ce_xCuO_4$ no incommensurate magnetism has been observed.[10] The difference in the spatial modulation experimentally observed in $La_{2-x}Sr_xCuO_4$ and $YBa_2Cu_3O_{6+y}$ has been related to a difference in the topology of the Fermi surface.[11,12]

From a theoretical side there has been a tremendous effort to describe the experimental situation and many schemes of calculation have been proposed; however, it is still not clear if one model is sufficient to describe all different materials. It is believed, on both experimental and theoretical grounds, that superconductivity and charge transport in high T_c cuprates are mostly confined to the CuO_2 planes;[13,14] so much attention has been dedicated to two-dimensional (2D) models that contain as an essential feature a competition between the band picture aspect and highly correlated many-body effects. The bonding combination of Cu and O orbitals ends up being quite deep below the Fermi level, so that no dynamical freedom is left to treat d and p orbitals separately[15] (there is some strong experimental evidence, mostly based on the study of the Knight shift, that in the CuO_2 plane one spin degree of freedom is observed[16]). Then the resulting complex can be described by a single-band Hubbard model.[17] Indeed, the applicability of the model to the superconducting copper oxide is related to the fact that upon doping most of these compounds exhibit a metal-insulator Mott transition.

Some evidence of incommensurate magnetic correlations was found in the 2D Hubbard model[18] and in the t-J model[19] by quantum Monte Carlo (QMC) calculations. To improve the situation the t-t' Hubbard model has been considered, but the results are not definite and there is no general agreement.[18–27] In the framework of a generalized random-phase approximation (RPA) it has been found[20] that for negative values of t' incommensurability starts developing at a finite hole density that increases from half filling as t' becomes more negative; for $t'=0$, $\delta(x)$ goes to zero when x goes to zero, but the values are much smaller than the experimental data. In Ref. 21 one- and three-band Hubbard models have been studied by RPA in the limit of infinite U; for $t'\neq 0$ incommensurability is found with $\delta(x)$ close to the experimental data in the region of low doping, but far for higher doping. In Ref. 22 the case of positive t' has been considered by QMC calculations at zero temperature; incommensurability is found, but with peaks in $S(\mathbf{k})$ moving along the diagonals in the Brillouin zone. In Ref. 23 exact diagonalization studies of the t-t'-J model have been performed; for negative values of t' incommensurability is observed with $S(\mathbf{k})$ moving along the diagonals, while for positive values of t' the peak in $S(\mathbf{k})$ remains at $\mathbf{Q}=(\pi,\pi)$ for all dopant concentrations studied. Other models that predict incommensurate spin fluctuations in $La_{2-x}Sr_xCuO_4$ are based on the use of nearly nested Fermi surfaces[24,25] and phase separation.[26]

By means of the composite operator method[28] (COM) we have computed the spin magnetic susceptibility $\chi(\mathbf{k},\omega)$ of the 2D single-band Hubbard model,[29] in the static approxi-

mation, where finite lifetime effects are neglected. In particular, the uniform static susceptibility $\chi_0(x,T)$ for various values of doping and temperature evidenced a striking qualitative agreement with the experimental situation in $La_{2-x}Sr_xCuO_4$.[30]

In this paper we shall study the evolution of the spin fluctuations on the doping concentration over the entire momentum spectrum. In the next section we review the main formula and present the results for the incommensurability amplitude. Some concluding remarks are given in Sec. III.

II. STATIC SUSCEPTIBILITY

The Hubbard Hamiltonian[17] is given by

$$H=\sum_{i,j} t_{ij}c^{\dagger}(i)c(j)+U\sum_i n_{\uparrow}(i)n_{\downarrow}(i)-\mu\sum_i c^{\dagger}(i)c(i). \tag{1}$$

The notation is the following. The variable i stands for the lattice vector $\mathbf{R}_i$. $\{c(i),c^{\dagger}(i)\}$ are annihilation and creation operators of c electrons at site i, in the spinor notation:

$$c=\begin{pmatrix} c_{\uparrow} \\ c_{\downarrow} \end{pmatrix}, \quad c^{\dagger}=(c_{\uparrow}^{\dagger}c_{\downarrow}^{\dagger}). \tag{2}$$

The fields $\{c(i),c^{\dagger}(i)\}$ satisfy canonical anticommutation relations

$$\{c_{\sigma}(i),c_{\sigma'}^{\dagger}(j)\}=\delta_{\sigma,\sigma'}\delta_{i,j},$$

$$\{c_{\sigma}(i),c_{\sigma'}(j)\}=\{c_{\sigma}^{\dagger}(i),c_{\sigma'}^{\dagger}(j)\}=0. \tag{3}$$

t_{ij} denotes the transfer integral and describes hopping between different sites; the U term is the Hubbard interaction between two c electrons at the same site with

$$n_{\sigma}(i)=c_{\sigma}^{\dagger}(i)c_{\sigma}(i). \tag{4}$$

μ is the chemical potential. In the nearest-neighbor approximation we write the hopping matrix as

$$t_{ij}=-4t\alpha_{ij}=-4t\frac{1}{N}\sum_{\mathbf{k}} e^{i\mathbf{k}\cdot(\mathbf{R}_i-\mathbf{R}_j)}\alpha(\mathbf{k}), \tag{5}$$

where for a two-dimensional square lattice with lattice constant a

$$\alpha(\mathbf{k})=\frac{1}{2}[\cos(k_x a)+\cos(k_y a)]. \tag{6}$$

The scale of the energy has been fixed in such a way that $t_{ii}=0$. It should be noted that since the interactions are restricted at the same site, the dimensionality of the system comes in only when a specific form for $\alpha(\mathbf{k})$ is taken. In other words, the stabilization of eventual cooperative phenomena is uniquely governed by the band dispersion.

We have shown[29] that in the static approximation the dynamical spin susceptibility is given by the expression

$$\chi(\mathbf{k},\omega)=\frac{2}{n^2-n-2D}[n(Q^R_{1111}+2Q^R_{1112}+Q^R_{1212})+(2-n)$$
$$\times(Q^R_{1212}+2Q^R_{1222}+Q^R_{2222})], \tag{7}$$

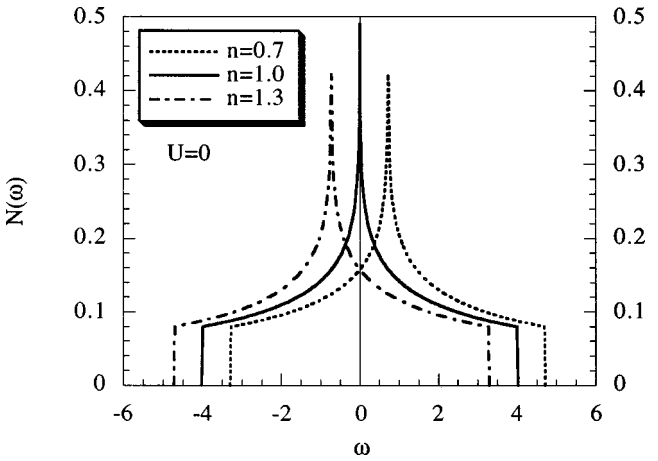

FIG. 1. Density of states $N(\omega)$ as a function of ω for various values of the doping. $U/t=0$.

where n is the particle density, D is the double occupancy, and by $Q^R_{\alpha\beta\gamma\delta}(\mathbf{k},\omega)$ we mean the retarded part of

$$Q_{\alpha\beta\gamma\delta}(\mathbf{k},\omega)=i\int\frac{d^2p\ d\Omega}{(2\pi)^3}G_{\alpha\beta}(\mathbf{k}+\mathbf{p},\omega+\Omega)G_{\gamma\delta}(\mathbf{p},\Omega). \tag{8}$$

The 2×2 matrix $G(\mathbf{k},\omega)$ is the thermal causal Green's function, defined by $G(\mathbf{k},\omega)=\langle T[\psi(i)\psi^{\dagger}(j)]\rangle_{FT}$, where FT denotes the Fourier transform. $\psi(i)$ is the doublet composite operator

$$\psi(i)=\begin{pmatrix} \xi(i) \\ \eta(i) \end{pmatrix}, \tag{9}$$

with

$$\xi(i)=[1-n(i)]c(i), \tag{10}$$

$$\eta(i)=n(i)c(i) \tag{11}$$

describing the transitions $(n=0)\Leftrightarrow(n=1)$ and $(n=1)\Leftrightarrow(n=2)$, respectively. By means of the equation of motion and by considering the static approximation, where finite lifetime effects are neglected, the Green's function $G(\mathbf{k},\omega)$ can be computed in the course of a fully self-consistent calculation where no adjustable parameters are considered.[28,29]

A. The noninteracting case

To better understand how the magnetic correlations are modified by the interaction, it is useful at first to consider the case of the noninteracting Hubbard model (i.e., $U=0$). The density of states $N(\omega)$, shown in Fig. 1, presents an energy band of width $\Delta(\omega)=8t$; the Fermi energy is situated at $\omega=0$ and the van Hove singularity (VHS) is at the center of the band. When $n<1$ the VHS is located at an energy $\omega_{\nu H}>E_F$; by increasing n,$N(\omega)$ shifts rigidly and $\omega_{\nu H}$ decreases; for $n=1$ the VHS lies at the Fermi energy; for $n>1$ we have $\omega_{\nu H}<E_F$. The Fermi surface (FS) is given in Fig. 2 for various values of n. By increasing n, the volume of the FS increases; for $n=1$ the FS is nested.

For noninteracting fermion systems, the spin magnetic susceptibility $\chi(\mathbf{k},\omega)$ can be expressed as

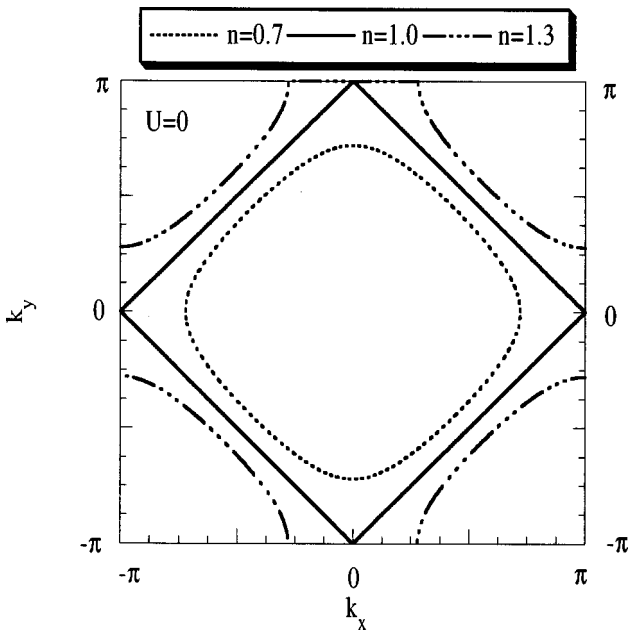

FIG. 2. Fermi surface for various values of the doping. $U/t=0$.

$$\chi(\mathbf{k},\omega)=-2\int\frac{d^2p}{(2\pi)^2}\frac{f(E(\mathbf{p}))-f(E(\mathbf{p}+\mathbf{k}))}{\omega-E(\mathbf{p}+\mathbf{k})+E(\mathbf{p})}, \quad (12)$$

with $E(\mathbf{p})$ and $f(E)$ being the energy spectrum and the Fermi distribution function, respectively. The static susceptibility $\chi(\mathbf{k})$ depends on the density of states and therefore on the position of the VHS; for a certain value of n and therefore for a certain value of ω_{vH}, $\chi(\mathbf{k})$ exhibits a maximum for a certain $\mathbf{k}^*$. When $n=1$ the VHS lies at the Fermi value and $\mathbf{k}^*=\mathbf{Q}=(\pi,\pi)$. On the other hand, when we have a nested Fermi surface there is a logarithmic divergence of the staggered susceptibility $\chi(\mathbf{Q})$ at low temperatures. It is a characteristic property of the free Hubbard model that for the same value of $n=1$ we have $\omega_{vH}=E_F$ and a nested Fermi surface. As a consequence, in addition to the divergence coming from the nested Fermi surface there is one coming from the VHS in the density of states and $\chi(\mathbf{Q})$ exhibits a stronger divergence than χ_0:

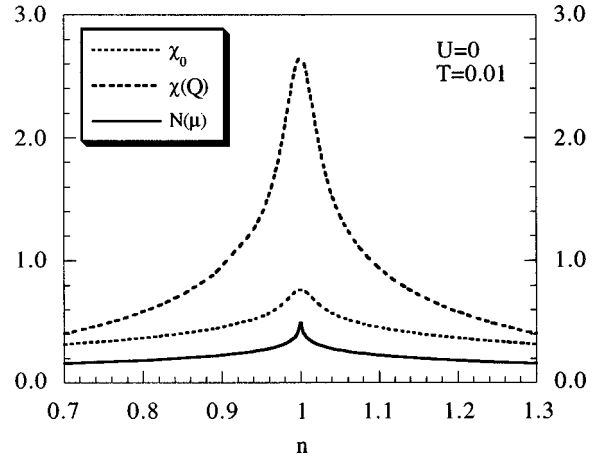

FIG. 3. $N(\mu)$, χ_0, and $\chi(\mathbf{Q})$ as functions of doping. $U/t=0$ and $k_BT/t=0.01$.

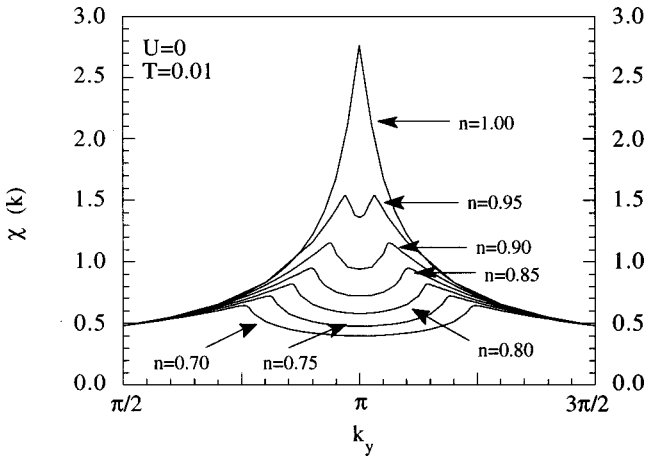

FIG. 4. Spin magnetic susceptibility $\chi(\mathbf{k})$ along the line $\mathbf{k}=(\pi,k_y)$ for $k_BT/t=0.01$ and various values of the doping. $U/t=0$.

$$\lim_{T\to 0}\chi_0\propto-\ln(k_BT/t), \qquad \lim_{T\to 0}\chi(\mathbf{Q})\propto-\ln(k_BT/t)^2. \quad (13)$$

In Fig. 3 we show $N(\mu)$, χ_0, and $\chi(\mathbf{Q})$ versus n. All these quantities exhibit a peak for $n=1$, due to the VHS; the stronger divergence exhibited by $\chi(\mathbf{Q})$ is due to the nesting of the Fermi surface. When $n\neq 1$ the Bragg peak at $\mathbf{Q}=(\pi,\pi)$ opens in four peaks, situated at $\mathbf{k}^*=[\pi(1\pm\delta),\pi(1\pm\delta)]$; there is a transition from commensurate to incommensurate magnetic correlations. In Fig. 4 we show $\chi(\mathbf{k})$ along the line $k_x=\pi, \pi/2\leq k_y\leq 3\pi/2$. The peaks exhibited by $\chi(\mathbf{k})$ are due to the VHS in the density of states; at half filling the VHS is at the Fermi value $\omega_{vH}=\mu$; when we move away from half filling the singularity moves:

$$\begin{aligned}&\omega_{vH}>\mu \quad \text{for} \quad n<1 \quad \text{(hole doping)}\\ &\omega_{vH}<\mu \quad \text{for} \quad n>1 \quad \text{(electron doping).}\end{aligned} \quad (14)$$

The behavior is completely symmetric due to the particle-hole symmetry of the model. The incommensurability amplitude $\delta(x)$ increases as a function of the doping $x=1-n$. This is shown in Fig. 5, where $\delta(x)$ is reported versus x. We also give the shift of the van Hove frequency with respect to

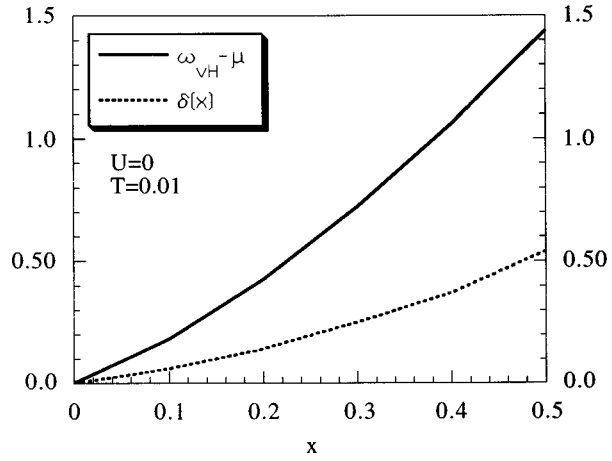

FIG. 5. $\omega_{vH}-\mu$ and $\delta(x)$ as functions of doping. $U/t=0$ and $k_BT/t=0.01$.

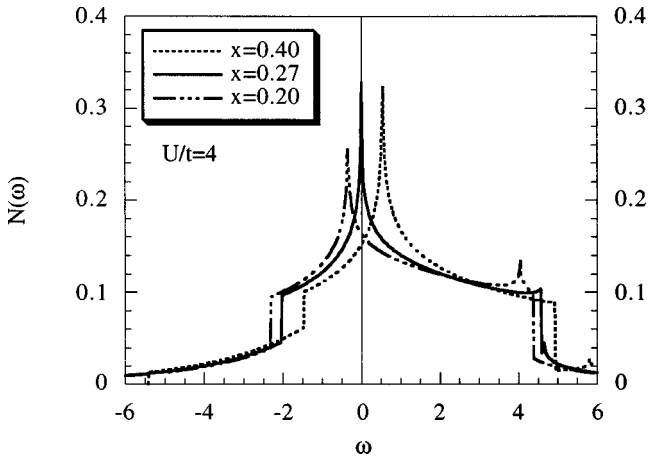

FIG. 6. Density of states $N(\omega)$ as a function of ω for various values of doping. $U/t=4$.

the chemical potential. It is interesting to observe that $\omega_{\nu H}-\mu$ and $\delta(x)$, when reported as functions of x, obey the same law:

$$\omega_{\nu H}-\mu \approx a x^{4/3}, \quad a \approx 3.62$$
$$\delta(x) \approx b x^{4/3}, \quad b \approx 1.31. \tag{15}$$

B. The interacting case

For the interacting case, owing to the Coulomb repulsion, two bands, the lower and the upper Hubbard bands, open in the density of states, as shown in Fig. 6. We see that by increasing doping the VHS moves across the Fermi energy, situated at $\omega=0$. Two VHS's appear: One has an energy $\omega_{1\nu H} \gg \mu$ and practically does not contribute; the other is close to the Fermi energy and there exists a critical value x_c of the doping such that

$$\omega_{2\nu H} < \mu \quad \text{for} \quad x < x_c,$$
$$\omega_{2\nu H} > \mu \quad \text{for} \quad x > x_c. \tag{16}$$

The value of x_c does not change with temperature and is determined by the ratio U/t, varying from 0 to 1/3 when U/t changes from zero to infinity; for $U/t=4$ we have $x_c=0.27$. The Fermi surface individuated by the lower-energy spectrum $E_2(\mathbf{k})$ is shown in Fig. 7. We see that the Fermi surface is nested for $x=x_c$.

The shifting of the VHS and the band structure effects have a drastic influence on the form of the susceptibility. Theoretical calculations performed show that around $\mathbf{Q}=(\pi,\pi)$ $\chi(\mathbf{k})$ has an incommensurate structure along the four corners of a square, with a minimum at $\mathbf{Q}$. This incommensurate structure contains a mixing of two components. The relative position and the intensity of the two contributions change significantly with doping. When the interaction is included, the $\mathbf{k}$-dependent susceptibility $\chi(\mathbf{k})$ can be written as

$$\chi(\mathbf{k})=\sum_{i,j=1}^{2} \chi_{ij}(\mathbf{k}), \tag{17}$$

where

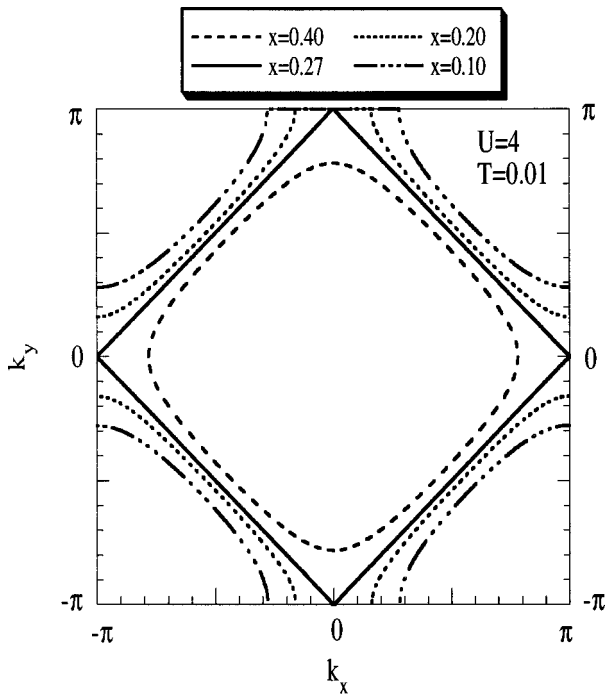

FIG. 7. Fermi surface individuated by the lower-energy spectrum $E_2(\mathbf{k})$ for various values of the doping. $U/t=4$.

$$\chi_{ij}(\mathbf{k})=\int \frac{d^2p}{(2\pi)^2} \frac{f(E_i(\mathbf{k}+\mathbf{p}))-f(E_j(\mathbf{p}))}{E_i(\mathbf{k}+\mathbf{p})-E_j(\mathbf{p})} K_{ij}(\mathbf{k},\mathbf{p}). \tag{18}$$

$E_1(\mathbf{k})$ and $E_2(\mathbf{k})$ are the upper and the lower Hubbard subbands and $K_{ij}(\mathbf{k},\mathbf{p})$ are expressed in terms of the spectral intensities. The explicit expressions for these quantities have been computed in the framework of the COM and are reported in Ref. 29. The term $\chi_{\text{inter}}=\chi_{12}+\chi_{21}$ describes the propagation of a spin accompanied by a spin excitation between the two bands $E_1(\mathbf{k})$ and $E_2(\mathbf{k})$, while the two terms χ_{11} and χ_{22} describe the propagation with a subsequent intraband spin excitation. Since E_1 takes values mostly above the chemical potential, the contribution of χ_{11} is small. The interband term χ_{inter} is shown in Fig. 8. This term originates

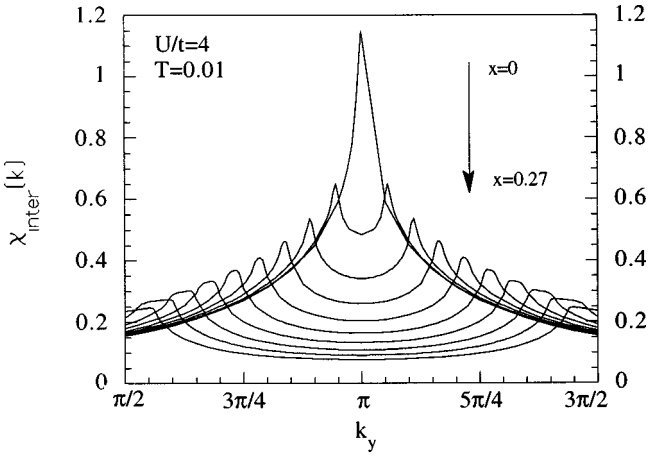

FIG. 8. Interband term $\chi_{\text{inter}}(\mathbf{k})$ along the line $\mathbf{k}=(\pi,k_y)$ for $k_BT/t=0.01$ and various values of the doping $x \leqslant 0.27$ with step 0.03. $U/t=4$.

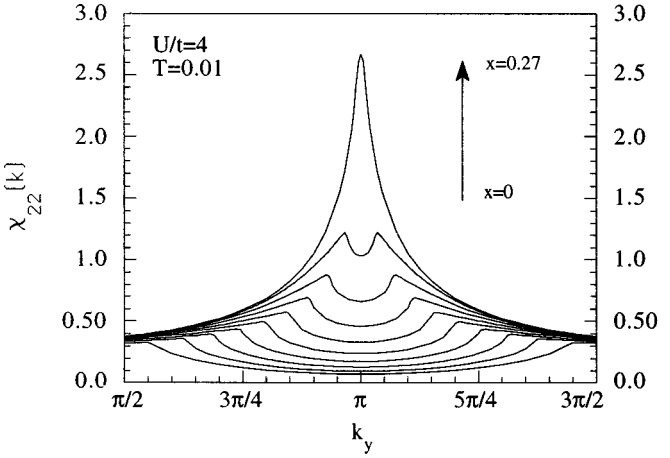

FIG. 9. Intraband term $\chi_{22}(\mathbf{k})$ along the line $\mathbf{k}=(\pi,k_y)$ for $k_BT/t=0.01$ and various values of the doping $x\leqslant 0.27$ with step 0.03. $U/t=4$.

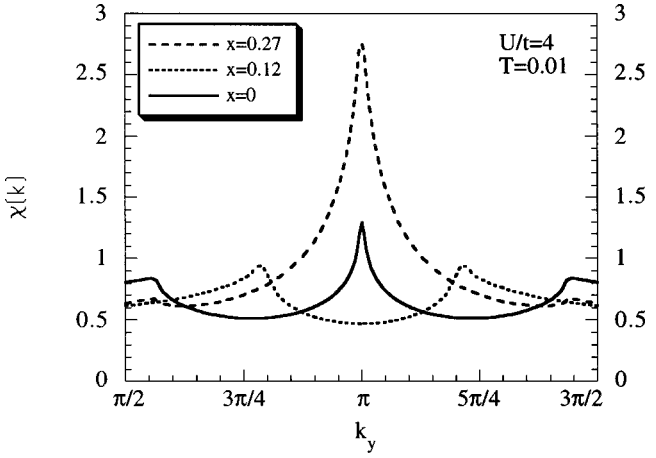

FIG. 11. Spin magnetic susceptibility $\chi(\mathbf{k})$ along the line $\mathbf{k}=(\pi,k_y)$ for various values of the doping x. $U/t=4$ and $k_BT/t=0.01$.

a peak in the susceptibility, which moves from the commensurate position $\mathbf{Q}=(\pi,\pi)$ to $(\pi,\pi/2)$ when the doping is increased from $x=0$ to $x=x_c$. The intensity of the peak decreases by increasing doping. The intraband term χ_{22} is shown in Fig. 9. This term gives a peak that is a reminiscent of the van Hove singularity in the density of states. At zero doping the VHS is far from the Fermi energy and the peak is located at $(\pi,\pi/2)$ and has a low intensity. When doping increases, the peak increases its intensity and moves along the line $(k_x=\pi,\pi/2\leqslant k_y<3\pi/2)$. At the critical doping $x=x_c$ the VHS lies at the Fermi energy determining a peak in the uniform static susceptibility, as reported in Fig. 10. Also, for $x>x_c$ we have a closed Fermi surface that becomes nested at $x=x_c$ and opens for $x<x_c$ (cf. Fig. 7). Then the peak of χ_{22} is situated at $\mathbf{Q}$ and has a very high intensity due to the concomitance of these two effects. It is interesting to note that the peak position of χ_{22} moves towards $\mathbf{Q}$ with the same law as given in Eq. (15). An enlarged Fermi surface with a volume larger than the noninteracting one has been shown by QMC calculations[27,31] and by other theoretical works.[32] The total susceptibility is shown in Fig. 11 for three values of doping. For zero doping we mainly have a commensurate structure with a peak coming from χ_{inter}, located at (π,π), and a smaller peak, coming from χ_{22}, located near $(\pi,\pi/2)$. Upon doping, the two peaks moves for different reasons. χ_{22} moves because the van Hove singularity moves towards the Fermi energy. χ_{inter} moves because the band structure changes with doping. When the critical doping $x=x_c$ is reached, the VHS is at the Fermi energy and the Fermi surface is nested. A commensurate structure is recovered with a very high peak coming from χ_{22}.

In Fig. 12 the incommensurability amplitude $\delta(x)$ is shown as a function of doping. In the region of low (high) doping the peak coming from χ_{inter} (χ_{22}) is predominant and very well separated from the other; in these regions $\delta(x)$ has been evaluated as the middle point of the half-width of the peak and we have a linear behavior. In the region $0.10\leqslant x\leqslant 0.18$ the two peaks overlap; $\delta(x)$ has been calculated by taking the average of both peaks and we have a plateau due to the superimposition of χ_{22} and χ_{inter}. For comparison we report the experimental data of Refs. 4, 5, 7, and 8. The linear behavior of $\delta(x)$, observed in the low-doping region, agrees exceptionally well with the experimen-

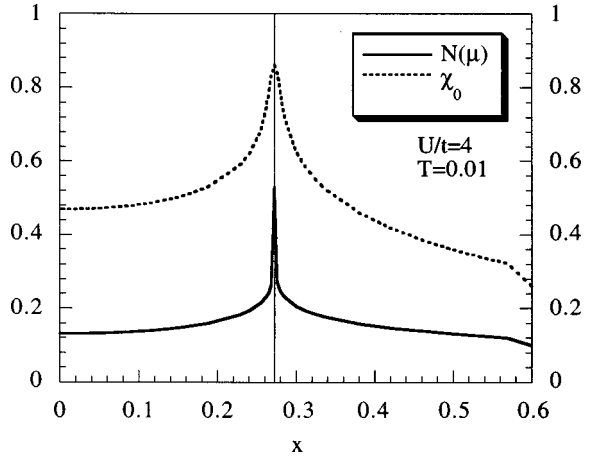

FIG. 10. Density of states at the Fermi energy $N(\mu)$ and the uniform static susceptibility $\chi_0(x,T)$ as functions of the doping x. $U/t=4$ and $k_BT/t=0.01$.

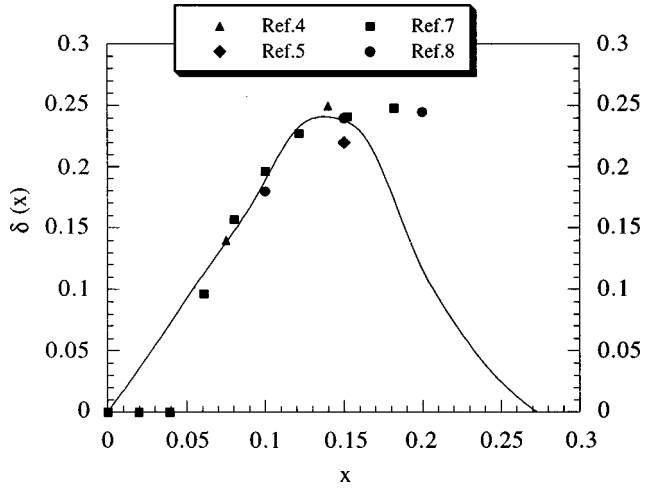

FIG. 12. Incommensurability amplitude $\delta(x)$ as a function of the doping x. The dashed line indicates the theoretical result. $U/t=4$ and $k_BT/t=0.01$.

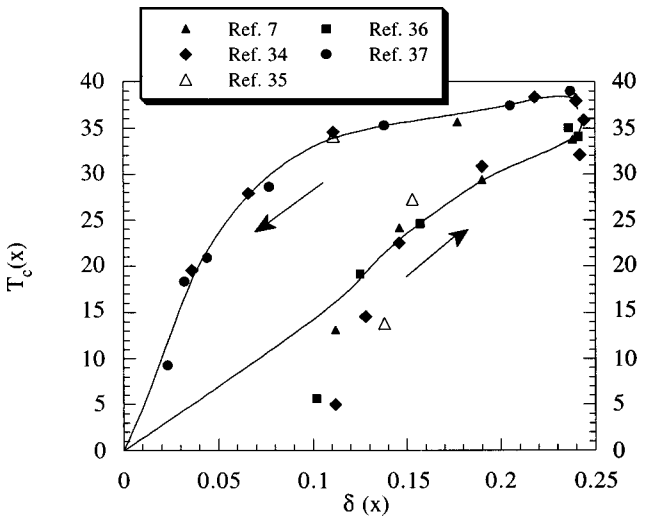

FIG. 13. Experimental values of T_c for $La_{2-x}Sr_xCuO_4$, taken from Refs. 7 and 34–37, versus the calculated incommensurability amplitude $\delta(x)$. The solid line is a guide to the eye.

tal data reported in Refs. 4–8; the downward deviation reported in Refs. 7 and 8 for $x>0.12$ might correspond to the plateau observed theoretically. It is important to stress that the calculated incommensurability amplitude $\delta(x)$ goes to zero only in the zero-doping limit because our analysis is restricted to a paramagnetic ground state.

The same result for $\delta(x)$ can be obtained by considering $\mathrm{Im}\chi(\mathbf{k},\omega)$. Some results have been given in Ref. 33. We preferred to study the **k**-dependent susceptibility $\chi(\mathbf{k})$ because this quantity provides more strict information about the spatial range of the magnetic correlations. On the other hand, an exact experimental determination of $\chi(\mathbf{k})$ is not easy since it must be calculated by the accessible $S(\mathbf{k},\omega)$ through a Kramers-Kronig relation.

One of the most striking features of the results presented in Fig. 12 is the resemblance between the incommensurability amplitude $\delta(x)$ and the critical temperature T_c. $\delta(x)$ is maximum in the region of optimal doping where T_c is maximum. It has already been experimentally observed in Ref. 7 that there is a linear relation between $\delta(x)$ and T_c up to the optimal doping level $x\simeq 0.15$. Our theoretical results confirm this behavior and show that a close similarity between $\delta(x)$ and T_c exists in the entire region of doping. This can be seen in Fig. 13 where experimental values for T_c, taken from Refs. 7 and 34–37, are reported versus the calculated incommensurability amplitude $\delta(x)$.

The present analysis shows that the interaction in the Hubbard model has mainly two effects. One is the change of the critical doping from $x=0$ to some critical x_c due to the shift of the VHS. This shift explains and reproduces well the unusual normal state behavior of χ_0 in hole-doped cuprates.[29,30,38] The other is a band-structure effect that is responsible for the incommensurate modulation of the magnetic susceptibility in the low-doping region.

The picture that emerges is that the magnetism probed by neutron-scattering experiments is correlated with the carrier density. In the low-doping region the susceptibility is mainly controlled by the term χ_{inter}, which describes band-structure effects and then reflects the topology of the Fermi surface. In the overdoped region the Fermi energy is close to the VHS and the effect of nesting in the intraband term is important. In $YBa_2Cu_3O_{6+y}$ we have a different topology of the Fermi surface and no nesting is expected; this might be the reason why incommensurability is not observed.

III. CONCLUDING REMARKS

The main results obtained in this paper are summarized as follows. There is experimental evidence that in hole-doped high-T_c cuprates the Fermi level is close to the VHS for values of doping close to those where the superconducting phase is suppressed. In the context of the Hubbard model a van Hove scenario describes well some of the unusual properties observed in the normal state, but our analysis shows that this scenario is related to the overdoped region and not to the optimal doping. The existence of a critical doping where the VHS lies at the Fermi energy should imply a peak in the staggered susceptibility. Then we predict that commensurate magnetism should be recovered in the nearness of the critical doping and beyond a close similarity between $\delta(x)$ and T_c in the entire region of doping. Recalling that in $La_{2-x}Sr_xCuO_4$ the commensurate-incommensurate transition is observed at the same value of doping $x\simeq 0.05$ where superconductivity starts, at least for $La_{2-x}Sr_xCuO_4$, a scenario[39] that relates the superconducting phase to the presence of incommensurate magnetism emerges.

Note added in proof. Incommensurate magnetic fluctuations have been recently observed[40] in $YBa_2Cu_3O_{6.6}$, with peaks along the diagonals of the Brillouin zone, starting from the M point. In the context of the Hubbard model, this situation can be described[41] by considering the hopping term along the diagonal of the plaquette (t-t'-U model).

ACKNOWLEDGMENTS

The authors wish to thank Professor M. Marinaro and Dr. A. Avella for many valuable discussions.

*Author to whom correspondence should be addressed. Electronic address: mancini@vaxsa.csied.unisa.it

[1] T. R. Thurston *et al.*, Phys. Rev. B **40**, 4585 (1989).
[2] G. Shirane *et al.*, Phys. Rev. Lett. **63**, 330 (1989).
[3] R. J. Birgenau *et al.*, Phys. Rev. B **38**, 6614 (1988).
[4] S. W. Cheong *et al.*, Phys. Rev. Lett. **67**, 1791 (1991).
[5] G. Shirane *et al.*, Physica B **197**, 158 (1994).
[6] K. Yamada *et al.*, Phys. Rev. Lett. **75**, 1626 (1995).
[7] K. Yamada *et al.* (unpublished).
[8] S. Petit *et al.* (unpublished).
[9] M. Tranquada *et al.*, Phys. Rev. B **46**, 5561 (1992).
[10] T. R. Thurston *et al.*, Phys. Rev. Lett. **65**, 263 (1990).
[11] J. Rossat-Mignod *et al.*, Physica B **169**, 58 (1991).
[12] R. Liu *et al.*, Phys. Rev. B **46**, 11 056 (1992).
[13] For a review see, e.g., S. Uchida, Jpn. J. Appl. Phys., Part 1 **32**, 3784 (1993); Z. X. Shen and D. S. Dessau, Phys. Rep. **253**, 1 (1995).
[14] E. Dagotto, Rev. Mod. Phys. **66**, 763 (1994).
[15] P. W. Anderson, Science **235**, 1196 (1987).
[16] A. P. Kampf, Phys. Rep. **249**, 219 (1994), and references therein.

[17] J. Hubbard, Proc. R. Soc. London, Ser. A **276**, 238 (1963).
[18] A. Moreo *et al.*, Phys. Rev. B **41**, 2313 (1990).
[19] A. Moreo *et al.*, Phys. Rev. B **42**, 6283 (1990).
[20] P. Bénard, L. Chen, and A. M. Tremblay, Phys. Rev. B **47**, 15 217 (1993); **47**, 589 (1993).
[21] Q. Si *et al.*, Phys. Rev. B **47**, 9055 (1993).
[22] N. Furukawa and M. Imada, J. Phys. Soc. Jpn. **61**, 3331 (1992).
[23] R. J. Gooding, K. J. E. Vos, and P. W. Leung, Phys. Rev. B **49**, 4119 (1994); **50**, 12 866 (1994).
[24] N. Bulut *et al.*, Phys. Rev. Lett. **64**, 2723 (1990).
[25] T. Tanamoto, H. Kohno, and H. Fukuyama, J. Phys. Soc. Jpn. **63**, 2739 (1994).
[26] V. Y. Emery and S. A. Kivelson, Physica C **235-240**, 189 (1994); J. M. Tranquada *et al.*, Nature (London) **375**, 561 (1995).
[27] D. Duffy and A. Moreo, Phys. Rev. B **52**, 15 607 (1995).
[28] F. Mancini, S. Marra, and H. Matsumoto, Physica C **244**, 49 (1995); **250**, 184 (1995).
[29] F. Mancini, S. Marra, and H. Matsumoto, Physica C **252**, 361 (1995).
[30] J. B. Torrance *et al.*, Phys. Rev. B **40**, 8872 (1989).
[31] N. Bulut, D. J. Scalapino, and S. R. White, Phys. Rev. B **50**, 7215 (1994); Phys. Rev. Lett. **73**, 748 (1994).
[32] D. M. Newns, P. C. Pattnaik, and C. C. Tsuei, Phys. Rev. B **43**, 3075 (1991); J. Beenen and D. M. Edwards, *ibid.* **52**, 13 636 (1995).
[33] F. Mancini, H. Matsumoto, and D. Villani, Czech. J. Phys. **46**, 1871 (1996).
[34] J. W. Loram *et al.* (unpublished).
[35] R. B. van Dover *et al.*, Phys. Rev. B **35**, 5337 (1987).
[36] M. W. Shafer, T. Penny, and B. L. Olson, Phys. Rev. B **36**, 4047 (1987).
[37] J. B. Torrance *et al.*, Phys. Rev. Lett. **61**, 1127 (1988).
[38] U. Trapper, D. Ihle, and H. Fehske, Phys. Rev. B **54**, 7614 (1996).
[39] F. Mancini, S. Marra, and H. Matsumoto, Physica C **263**, 70 (1996); F. Mancini, V. Oudovenko, and D. Villani, Czech. J. Phys. **46**, 1873 (1996).
[40] P. Dai, H. Mook, and F. Dogan, cond-mat/9707112(unpublished).
[41] A. Avella, F. Mancini, and D. Villani, Phys. Lett. A (to be published).